BRAKING TORQUE METER

Development of the momentum measuring device for process control in motor production industry

Ilia Kemppi
Sergei Ossif

Metropolia University of Applied Sciences
Helsinki, Finland, 2014

Power and productivity for a better world™

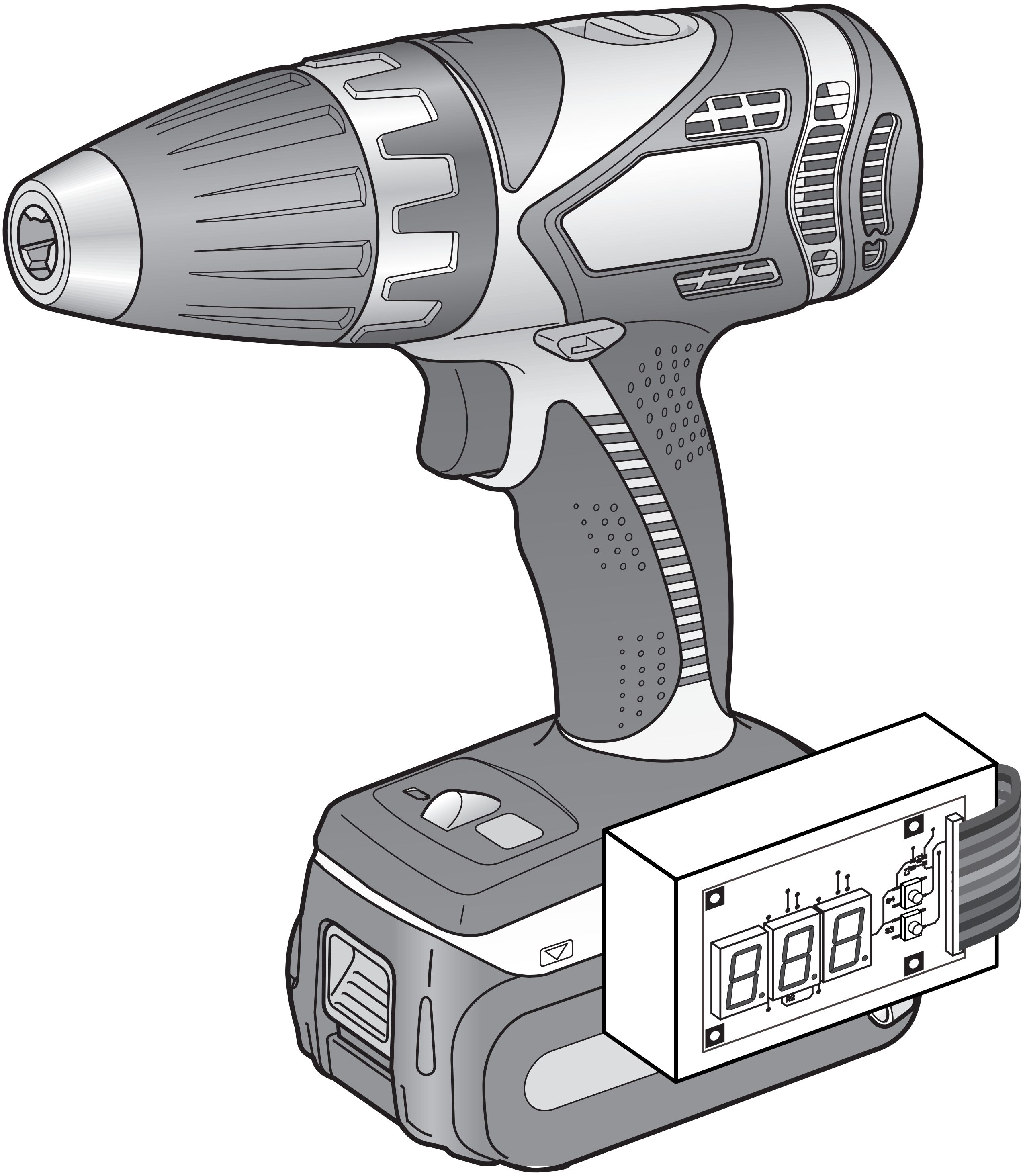

Abstract

In this project we were assigned to design, assemble and implement a braking torque measurement device. Coil taping machines on ABB Drives production line should have precisely calibrated brakes to put isolation properly. Portable calibration device for factory use is developed on a base of cordless drill infused with a current shunt wire. Torque to current characteristic of the drill motor was found to be linear. Model of the torque response was approximated and implemented on a small microcontroller-based device. Powered from the drill battery, the device is equipped with filters, amplifiers and a large LED screen, where braking torque of the shaft is shown in Newton-meters. Measurement range of the device reaches up to 4 Nm with precision of 0.05 Nm.

Abbreviation list

ADC - Analog-to-digital converter

ASIC - Application-specific integrated circuit

DC - direct current

DSP - digital signal processing

EMI - electromagnetic interference

RPM - revolutions per minute

PCB - printed circuit board

PWM - Pulse-Width Modulation

μC - microcontroller

SPDT - Single pole double throw (switch)

SMD - Surface-mount device

Contents

List of Figures

1 Introduction

Stator coil insulation is an important step in the production of electric motors. Motor life is dependent on the aging of insulation materials and on overall insulation quality.

Figure 1.1: Stator coils

During stator manufacture, winding coils are covered with several layers of insulation tape. On a particular ABB Oy Drives factory, automated insulation machine rotates two rolls of tape around the hairpin. As it moves along the conductor piece, tape overlaps in spiral manner and forms a layer of insulation material on the coil.

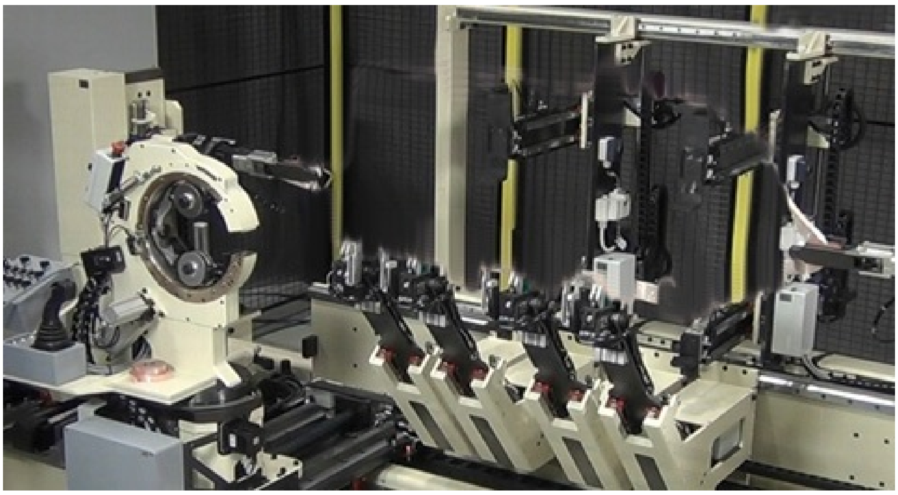

Figure 1.2: Coil insulation machine

Important part of this process is to provide constant amount of tension on the tape, as it wraps tightly around the piece. For this, tape holder has special brakes which oppose its free rotation. If tension is too low, insulation will be done improperly. Too high tension will wear the winding machine down if not damage it. The amount of turns at a time also affects the tape tension. When fresh roll is loaded in the machine, it takes more than two full turns of insulation head around the coil before tape roll unwinds once. When the roll is almost depleted, it unwinds one turn at a time together with insulation head. In order to achieve proper insulation, optimal level of braking torque should be provided on the tape shaft in both cases.

For this, insulation winding machine has mechanical feedback tip which slightly touches the tape roll. From the diameter of the roll, brakes are automatically adjusted by some pre-set ratio. Some kind of torque measuring instrument is required to check if the insulation machine breaks need correction. Solution should also be portable enough to examine several machines. Decision has been made in the direction of electronic device based on the cordless drill. By hacking into its power circuitry, it should be possible to find out the drilling load.

Figure 1.3: Panasonic EY7441 drill

For the project, we have been provided Panasonic EY7441 portable battery drill. It has brushed DC motor with permanent magnet stator and a gearbox with two nominal speeds of 400 RPM (LOW gear) and 1400 RPM (HIGH gear). Rotation speed within these limits is precisely controlled with the trigger. Gearbox also has directional switch and torque limiter. Operating voltage of the drill motor is 14.4 Volt.

2 Theoretical background

Energy in electrical motor is governed by following equation, which relates mechanical and electrical power:

$$V \cdot I = P_{motor} = k \cdot \omega \cdot T$$

with k being electromechanical constant.

When DC motor is energized, the reaction of the stator magnetic flux with rotor armature current produces a torque that forces armature to rotate [1]. This relation is described as following

$$\tau = k \cdot \phi \cdot i_a$$

where k is some motor-specific constant.

DC motors with permanent magnet stators exhibit good linearity of this characteristic, because magnetic flux is constant and does not depend on the electrical power. Reactive part of the armature impedance causes nonlinearity during fast current transitions, but with constant load to the motor, the power equation comes to equilibrium and the current exhibits linear dependence to the torque from the shaft. Because of minuscule differential voltages on the input, shunt low pass filter is Digital measurement devices in principle use analog-to-digital converter for sampling the voltage readings with certain precision. In order to get the value of the current, a resistor should be introduced between supply and the load (high-side current shunt). Motor current when passed through the shunt will produce a voltage proportional to the shunt resistance. The resistivity of the shunt should not be too small nor too big for it to produce voltage enough for adequate readings without disturbing the system.

By replacing the current in the torque formula by shunt voltage V_{shunt} over its resistance R_{shunt} and introducing the quantified voltage, taken from the ADC by number of bits n_{adc} times resolution V_q, we get following relation:

$$i_a \leftarrow \frac{V_{shunt}}{R_{shunt}}$$

$$V_{shunt} \leftarrow V_q \cdot n_{adc}$$

$$\tau = k \cdot \phi \cdot \frac{V_q \cdot n_{adc}}{R_{shunt}}$$

By grouping all the constants together, one constant coefficient K can be used instead:

$$\tau = \left[\frac{V_q \cdot k \cdot \phi}{R_{shunt}}\right] n_{adc} = K \cdot n_{adc}$$

The coefficient K for a particular motor can be directly derived from ADC data, when load torque is known.

3 Drill characteristics evaluation

Shunt sensing system

In order to measure current passing to the motor, a thick copper wire with resistance 0.01 Ohm was added as a shunt resistor between battery and the trigger, replacing the initial conductor from the drill assembly. Resistance of the shunt wire was measured using precision ohmmeter. Observed resistance produces voltage drop enough for measuring the current while thickness prevents insulator melting due to heat dissipation.

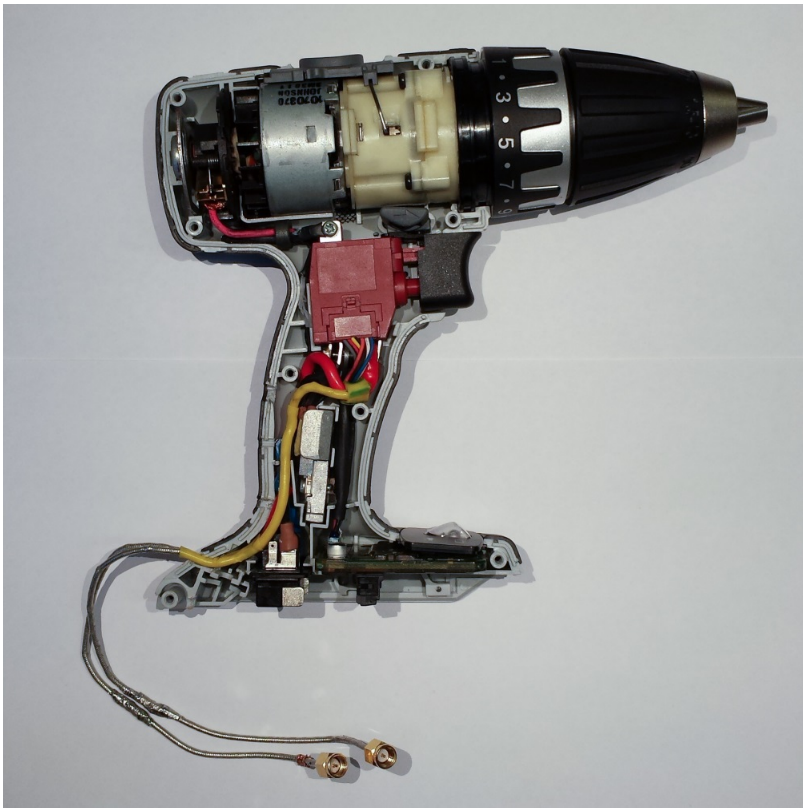

Figure 3.1: Panasonic EY7441 drill disassembled

Probes are connected to both nodes of the shunt resistor. As the drill motor produces strong EMI, braid-shielded coaxial cables were selected to minimize the noise. Both cable shields are connected to the battery ground in order to maximize shielding effectiveness. SMA coaxial connectors are used for connection to the measurement equipment.

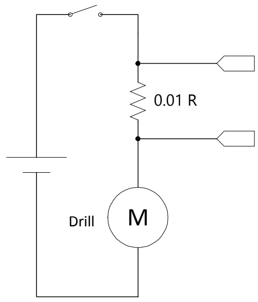

Figure 3.2: Shunt sensing system diagram

From the probes, it has been found out that trigger controls rotation speed of the motor with PWM: depending on the trigger position, pulse width is changing. When trigger is fully depressed (full speed), PWM is replaced with plain DC flowing into the motor. This dramatically simplifies the measurements in full speed conditions. However, a significant amount of noise is coupled onto the shunt resistor and probe wires, which calls for particular measures described in following chapters.

Measurement interface

To prove the theoretical model and plot the drill performance, sample measurements were made with an ADC and logging software. Figure 3.3 contains simple diagram of the measurement interface.

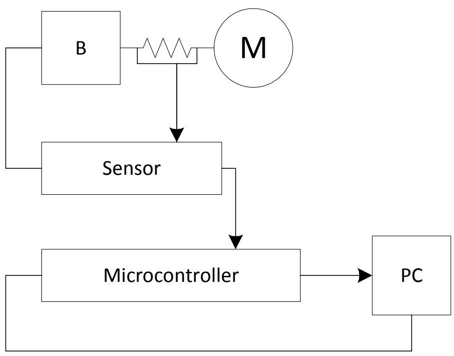

Figure 3.3: Measurement interface block diagram

From the shunt probes, voltage signal is preconditioned in the sensor module and fed directly into integrated ADC of microcontroller. Then, analog data is sampled, converted and transmitted to the PC through serial connection where it is logged into a file for later analysis.

As an ADC microcontroller solution, Texas Instruments MSP430 Launchpad development board was selected for its compact size and ease of deployment.

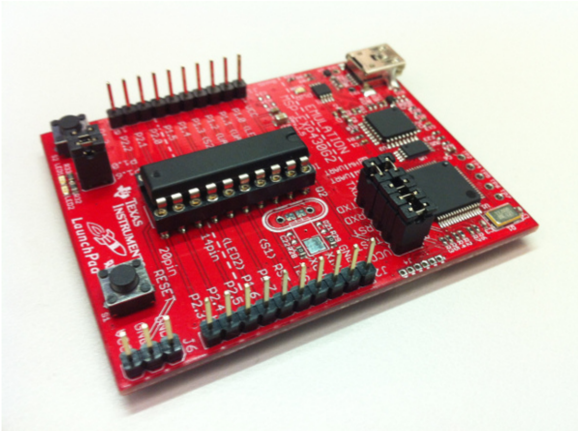

Figure 3.4: TI MSP430 Launchpad

MSP430G2553 microcontroller, featured on the development board, has fast 16-bit processor and 10-bit ADC. Together with Launchpad, it is possible to set up serial RS-232 connection to PC via USB interface. Development board is powered from USB port; microcontroller gets 3.6 Volt from the voltage regulator.

To prevent EMI generated by the drill motor from entering the sensing circuitry, metal enclosure for the development board was cut and folded from a tin can. Unfolded blueprint of the metal box is presented in figure 3.5.

Two apertures from the left side are to fit in SMA connectors, and next to it big opening for USB cable connector is made by overlapping two apertures. Slot at the right side matches reset button position on the development board. Power indicator on the Launchpad (green LED) could be seen from aperture at the long end of the box. From inside, box is insulated with tape. Soft foam is glued to the walls to reduce vibration and fix the contents in place.

To maximize the shielding effectiveness, enclosure is connected to the battery ground via probe shields. The whole sensing assembly is then attached on the bottom of the drill accumulator, furthest place from the motor.

Sensing circuitry

Preconditioning of the signal before ADC reading consists of following steps: filtering, isolation and scaling. All of these steps are implemented on the same com-

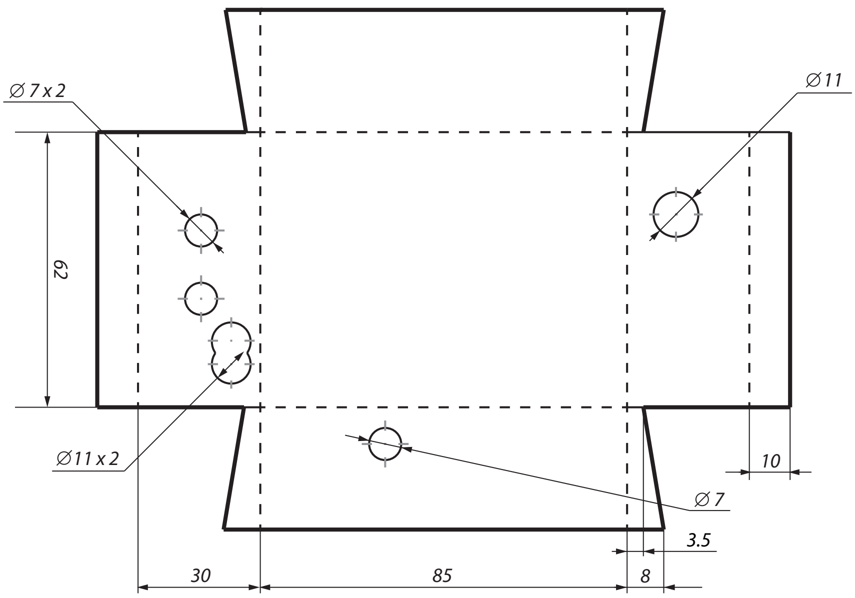

Figure 3.5: Enclosure box template

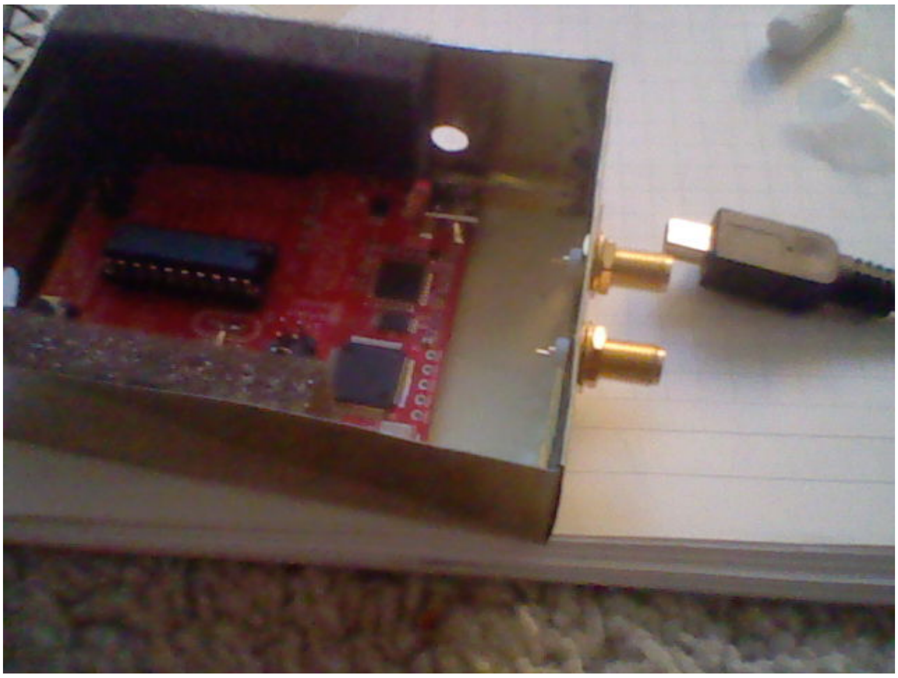

Figure 3.6: MSP430 Launchpad inside the box

pact circuit board, while battery's voltage supply and ground are taken from the highest probe and the cable shield respectively.

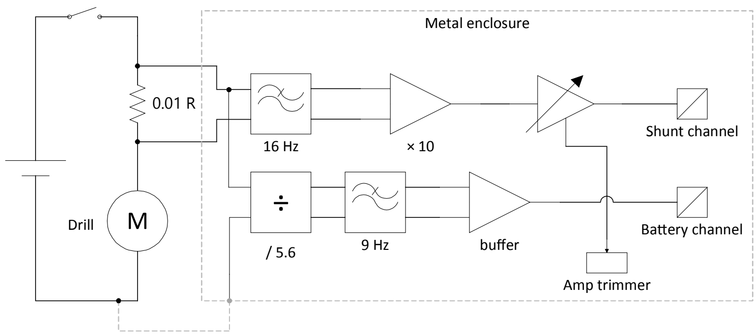

Figure 3.7: Signal preconditioning system

Passive low-pass filter of first order with cut-off frequency at 16 Hz eliminates high-frequency noise, leaving mostly DC component from the voltage on shunt. Signal isolation is performed with special AD8210 current sensing amplifier by Analog Devices. This ASIC solution includes special instrumentation amplifier with adjustable rails and fixed amplification factor of 20 dB. Additional amplification stage with negative feedback is added before ADC channel. Amplification is implemented on TS922 dual rail-to-rail amplifier by STMicroelectronics. Feedback gain can be controlled with potentiometer in order to match the dynamic range of the amplified shunt voltage to the ADC dynamic range being 3.6 Volts (Launchpad digital supply).

With two shunt probes from the positive side of the motor, battery voltage can be measured with another ADC channel, by taking voltage level from the highest probe in respect to the ground. Panasonic EY7441 nominal accumulator voltage being 14.4 Volts actually varies depending on the charge left. Fresh charge of the device corresponds to almost 17 Volts, which is certainly off ADC limits (3.6 Volts). Simple resistive voltage divider in kilo-Ohm range is used to scale the sensing voltage down by factor 1/5.6, so that it does not exceed the ADC power supply. After the divider, passive low pass filter with cutoff frequency at 9 Hz and voltage follower are placed in order to isolate and filter the sensing signal.

Due to gain saturation at near supply voltages in both amplifiers of the circuit, sensor board will get 5 Volt supply from separate voltage regulator. Dynamic range of the shunt voltage is kept in the range of 3.6 Volt with a potentiometer.

Linear dropout regulator of 7805 series is used to provide 5 Volts from the drill accumulator supply. Two electrolytic bypass capacitors are present in case of quick

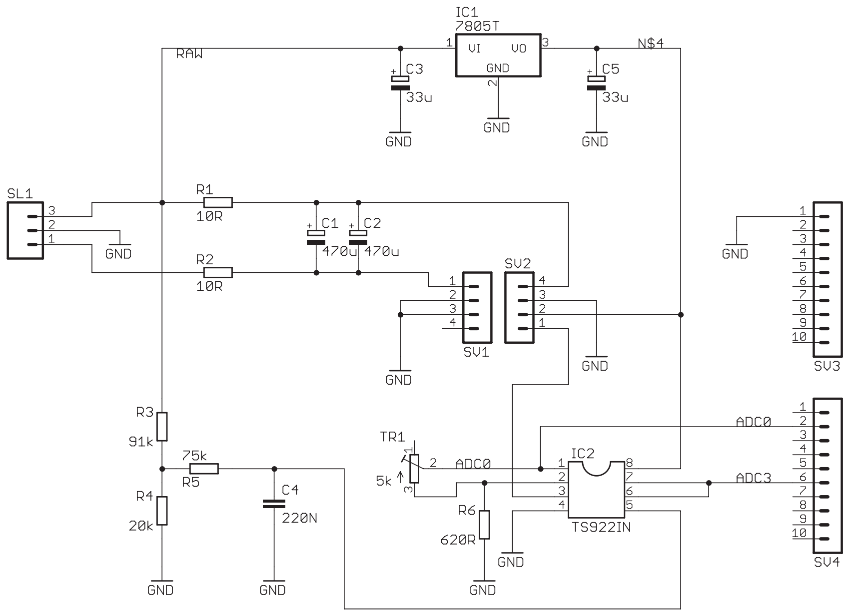

Figure 3.8: Sensor board circuit diagram

transients due to motor operation. AD8210 breakout board is inserted in two pre-aligned 4-pin slots.

Because of minuscule differential voltages on the input, shunt low pass filter is designed with large electrolytic capacitors for least amount of series resistance. In contrast, minimum footprint filter is used for battery sensing channel, as its voltage is not much affected by series resistance.

Grounds of development board and sensor circuit are interconnected as the common reference. ADC0 channel is used for shunt measurements and ADC3 is for battery measurements.

Both copper layers of the board are ground planes meant to decouple possible high-frequency noise and improve the ADC readings. SMD chip resistors and capacitors are placed on the bottom layer to save space.

From the interior side of probe connectors, **signal wires are inserted to the green screw terminal in following order (left to right): low side probe, ground, high side probe.**

Galvanic connection and mounting onto development board is made with two 10-pin female sip connectors, which are aligned to fit the Launchpad expansion pins. Negative feedback trimmer is placed to match the reset button enclosure slot, allowing to tune the second stage gain without disassembling the device.

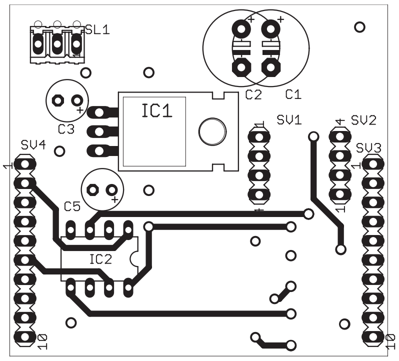

Figure 3.9: Sensor board top layout

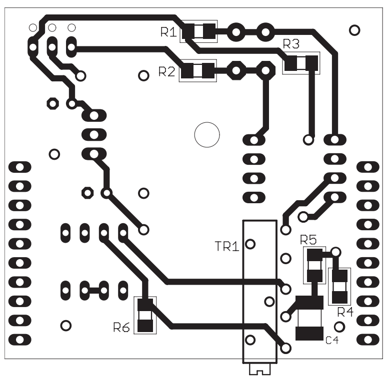

Figure 3.10: Sensor board bottom layout

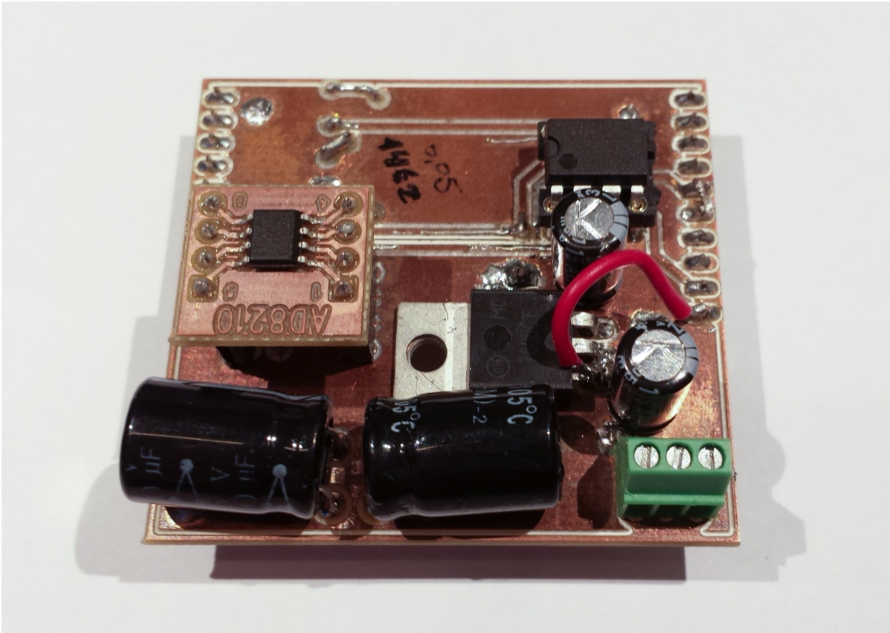

Figure 3.11: Assembled sensor board, top view

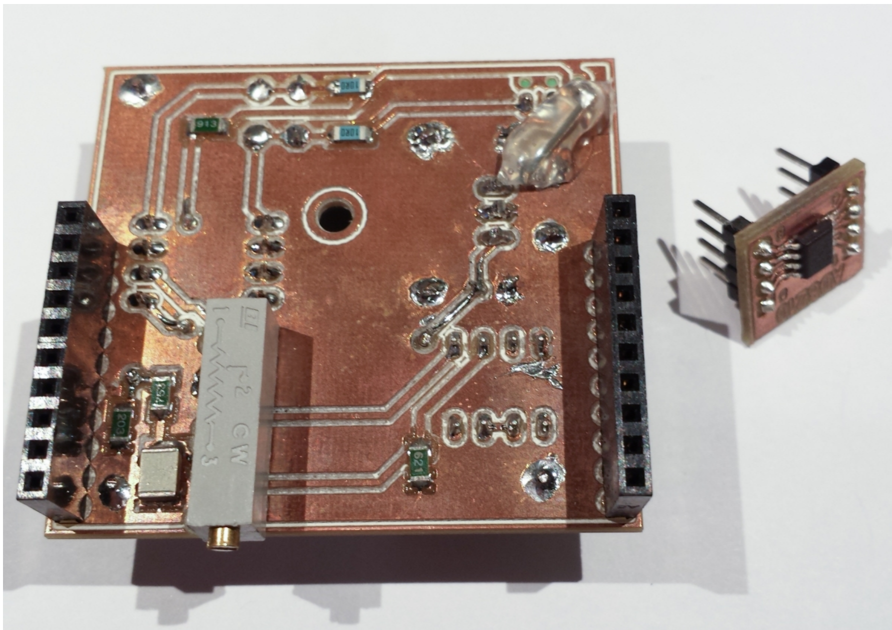

Figure 3.12: Assembled sensor board, bottom view

Torque machine measurements

Simple microcontroller logging program was developed for data acquisition. Readings, gathered from each ADC channel are collected and averaged 1024 samples at a time. Together with the torque level indicator, these are refreshed and translated into PC serial port each second.

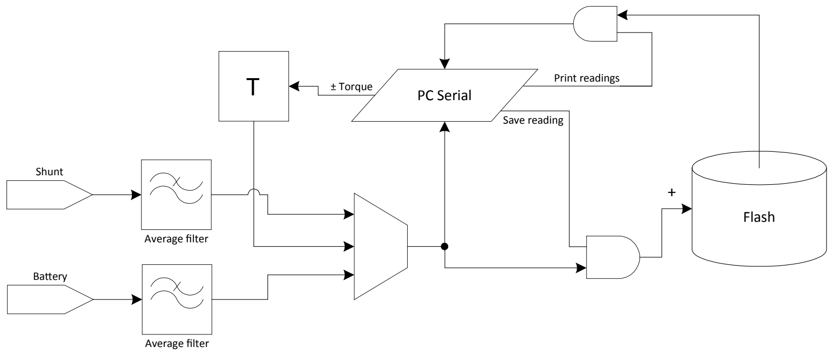

Figure 3.13: Sampling program data diagram

Depending on the braking force applied to the drill shaft, person in charge of measurements will increment or decrement the value of the torque level indicator by pressing buttons in the PC serial port application. In order to keep only actual measurement data and discard all the standby and transition values from the list, momentary data samples can be selected. This is the example of serial port output:

```
Torque: 9 Shunt: 457 Battery: 730
Torque: 9 Shunt: 457 Battery: 729 +
Torque: 9 Shunt: 456 Battery: 729
Torque: 9 Shunt: 457 Battery: 728 +
Torque: 9 Shunt: 455 Battery: 728
Torque: 9 Shunt: 457 Battery: 727
Torque: 9 Shunt: 457 Battery: 726
Torque: 9 Shunt: 458 Battery: 726 +
Torque: 9 Shunt: 460 Battery: 725
```

Lines with plus symbol are saved into internal flash memory of the microcontroller. This prevents data loss in case if Launchpad will get disconnected. When desired amount of samples is collected, flash memory can be printed into the terminal in comma-separated value format:

```
Acquired data:

0, 296, 747
0, 295, 745
0, 293, 742
5, 385, 720
5, 384, 718
5, 384, 717
9, 471, 698
9, 473, 696
9, 471, 695
12, 517, 682
12, 514, 681
12, 514, 680
17, 603, 657
17, 605, 656
```

Measurements of ADC to torque characteristics were carried out on the torque generator machine in the power electronics laboratory of Metropolia UAS. Measurements were made using HIGH gear of the drill to narrow the torque range and increase the precision. Gain of the second amplification stage in the shunt channel was set to match the motor lock position (stall torque) to the value of about 900 ADC bits (from 1023 being maximum).

After dynamic range has been tuned, several measurements were made by braking the spinning drill with the torque generator from free-run till lock position. With torque increased, current flowing into the system increased as well, heating up the motor noticeably. High-torque operation drains battery relatively fast, and after couple of full-range tests, battery was depleted.

All collected data points have demonstrated that dependence of the motor current on the load torque is *linear and does not depend on the battery voltage whatsoever*. From different tests with various battery charge levels, data trend has provided almost the same slope with minimum deviation. Drill motor characteristics is approximated from combined readings with first-order model (Figure 3.14):

MATLAB Curvefit tool was used to provide the following data model:

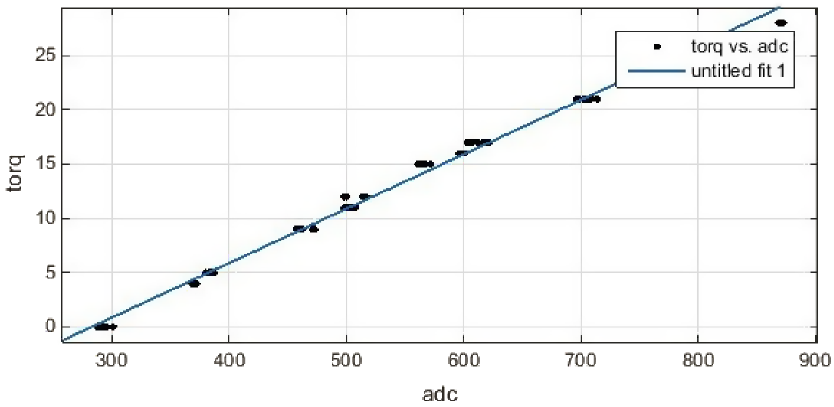

Figure 3.14: Braking torque against ADC readings

```
Linear model Poly1:
     f(x) = p1*x + p2
Coefficients (with 95% confidence bounds):
     p1 =     0.05008  (0.04934, 0.05081)
     p2 =       -14.1  (-14.52, -13.69)

Goodness of fit:
  SSE: 33.64
  R-square: 0.9946
  Adjusted R-square: 0.9946
  RMSE: 0.5829
```

where p2, being the 1st order polynomial constant coefficient, is the torque generator free-running load:

$$T \approx 0.05 \cdot n_{adc} - T_{free}$$

In conclusion, these results prove linearity of the motor characteristic, predicted earlier in the theoretical part. High computing power is not required when computing polynomial equations of first order. This, and independence from the battery voltage simplifies development of autonomous measuring device. Basic ADC capable microcontroller can handle the calculations, while batteries of various capacities can be used without disturbing the measurements.

4 Portable device development

Standalone system

Purpose of autonomous measurement system is to provide computational platform for the sensing circuitry while being powered from the drill battery.

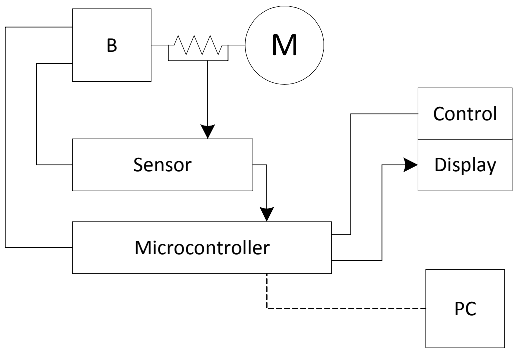

Figure 4.1: Autonomous measurement system

Display and possibility of user interaction are vital for the digital measurement device. These will be put to exterior of the metal enclosure, while keeping sensing circuitry shielded.

Microcontroller board

The μC board was designed to replace the existing solution with MSP430 Launchpad. While it was working quite well, the idea was for the device to be portable and the Launchpad couldn't provide it without an external 5 V power supply. To keep the compatibility with the sensor board, the spacing of the SIP connectors should remain the same. To achieve that, the original schematic and board design were downloaded from Texas Instruments web-site [2]. Everything from the original schematic, except the DIP10 connector, 2 SIP10 connectors were removed and the existing schematic was built around these constraints.

To convert 14.4 V from battery into usable 3.3 V for the μC, LM350 was chosen. It is an extremely reliable adjustable voltage regulator and provides excellent performance while keeping BOM cost down. LM350 provides output current up to 3A and line regulation of 0.015%/V which is very convenient as the precision of the μC's ADC depends on the stability of the VCC line.

For the display board we use 3 7-segment display. To connect it directly it needs 24 control lines, which is a lot more than we can afford. To work around this a very simple multiplexing was implemented.

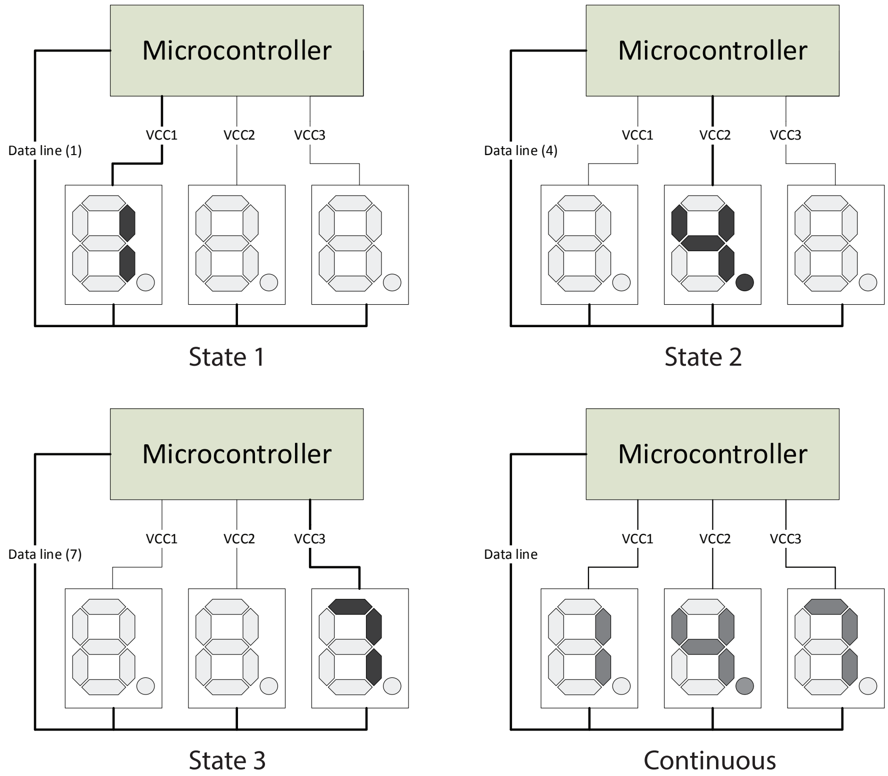

Figure 4.2: Multiplexing: general idea

The idea is to use 3 NPN transistors to drive only one display at the time. Also the decimal point was hardwired to the VCC line. As the result, we only need 7 control lines for 7 segments and 3 control lines to switch between the display. The switching speed must be high enough, so that the human eye is not able to notice flickering, but not too high to affect the firmware's performance.

As the power consumption in order of dozens of mA, BC817 is a good choice. It comes in a tiny SOT23 package and allows for up to 500mA of collector current.

We used 14 pin connector to connect to the display board. It used for:

- 7 signal lines to drive individual segments
- 3 power lines to drive individual screen
- 2 signal lines for RST and ZERO button
- 2 for general ground and power line

At the back of the board there is a 6 pin debug connector. It makes possible to program and reprogram the μC without disassembling the device and also provides TX and RX lines for UART communication.

The board was manufactured with Metropolia inhouse production room using LPKF PCB milling machine. Traces were tinned with solder to protect copper from corrosion. At the bottom of the board 4 blobs of thermoplastic adhesive were added to ensure that bottom pins are not in contact with the box.

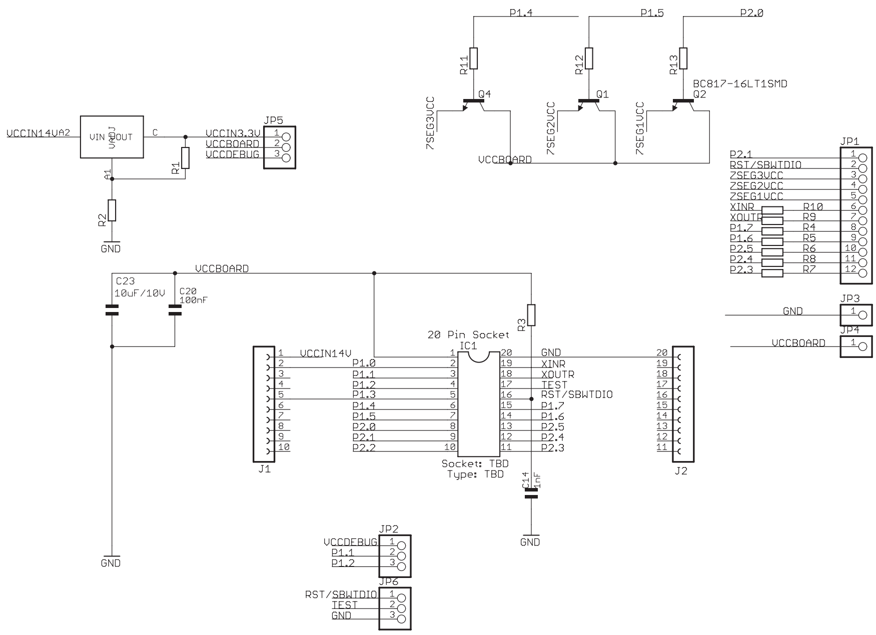

Figure 4.3: μC board schematic

Display board

As most of the functionality is done on the μC board, the display boards is extremely simple. There are only 3 7-segment screens, 2 buttons, 1 resistor and 14-pin connector.

The top button is used to set the reference to the current value. The bottom button resets the μC. Also there is a possibility to attach a plastic guard, which is fixed with 4 screws.

Complete assembly

For standalone operation shielding box was insulated inside and outside with duct tape. Bottom of the box has aluminium extension to fit into belt hook slot of the drill.

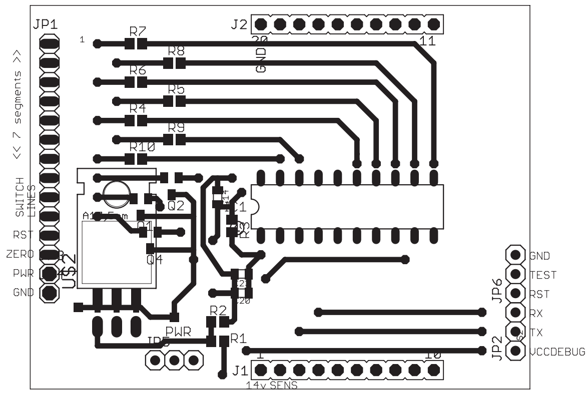

Figure 4.4: μC board PCB layout: top layer

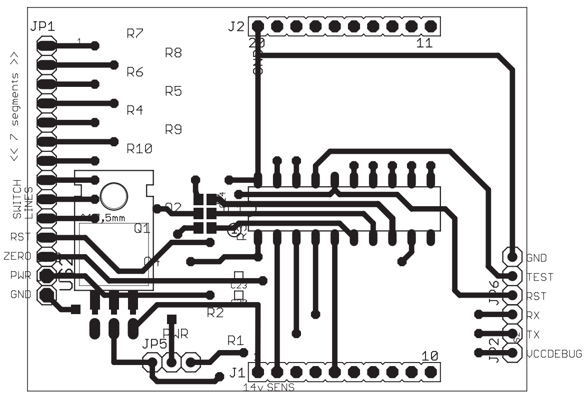

Figure 4.5: μC board PCB layout: bottom layer

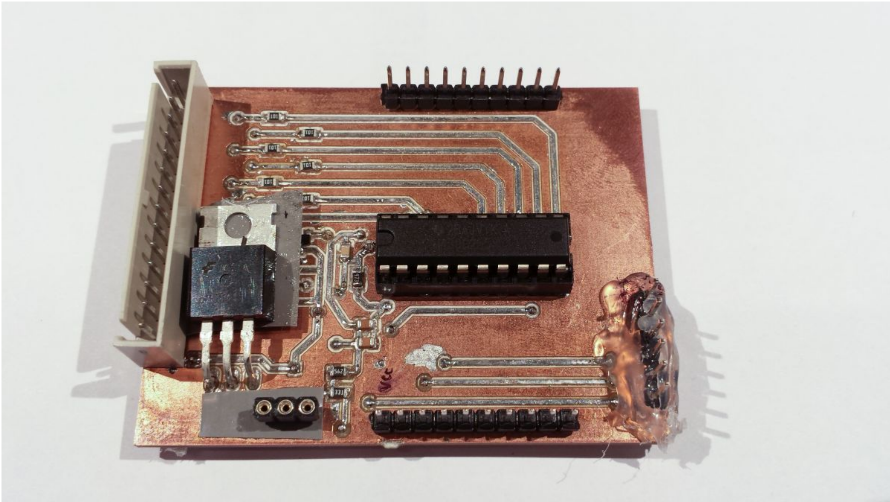

Figure 4.6: μC board assembled: top view

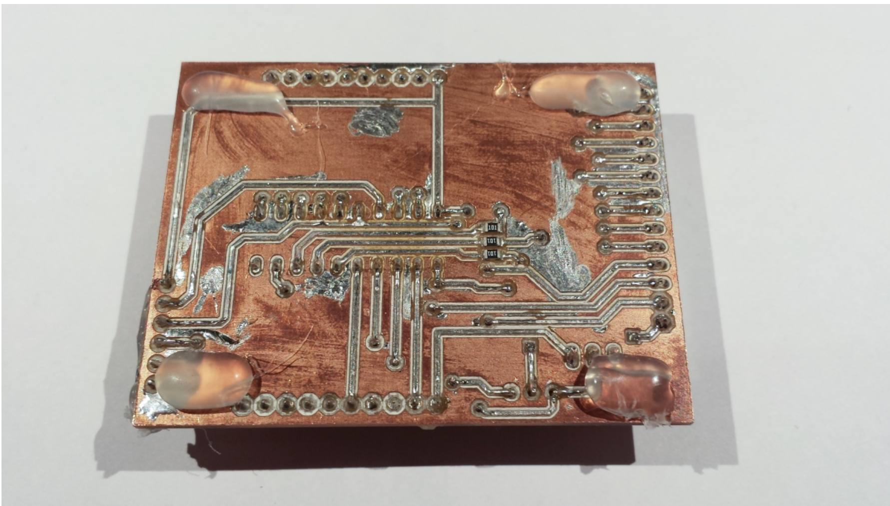

Figure 4.7: μC board assembled: bottom view

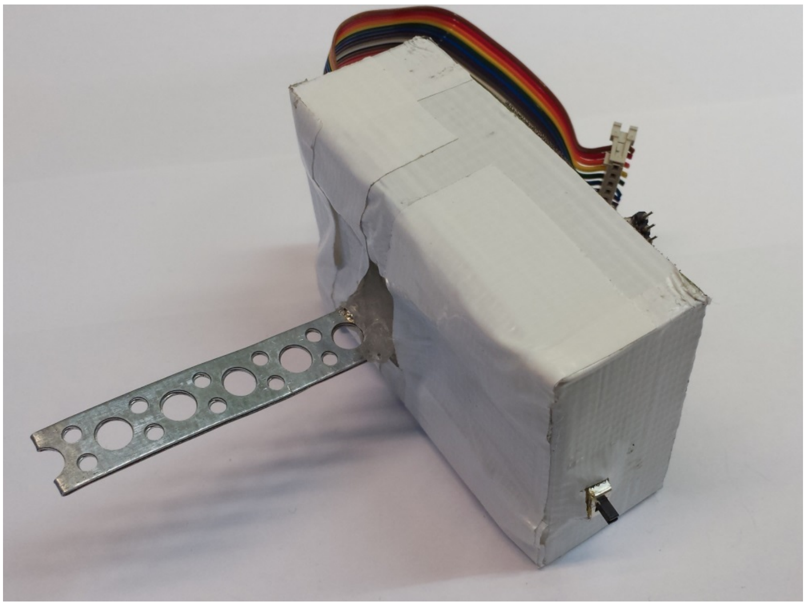

Figure 4.8: Shielding box, side view

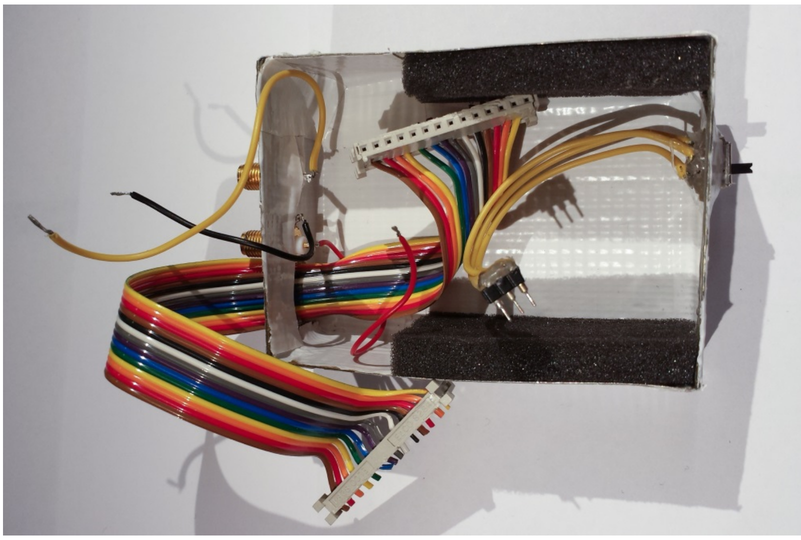

Figure 4.9: Shielding box, top view

14-pin ribbon cable is connected through former USB cable slot. Aperture which was used for reset and gain adjustment has been sealed with SPDT connector which expands the microcontroller board power selector. Switch position determines the board power source: either it's PC via programming interface or drill accumulator.

Measurement device is assembled in the following steps:

- Microcontroller board is placed onto bottom of the box.
- Display and power switch cables are connected onto the board.
- Sensor board is connected on the microcontroller board.
- Shunt signal wires are inserted into the sensor board, as described in the chapter "Sensing circuitry".
- Box lid is closed and display board connected.

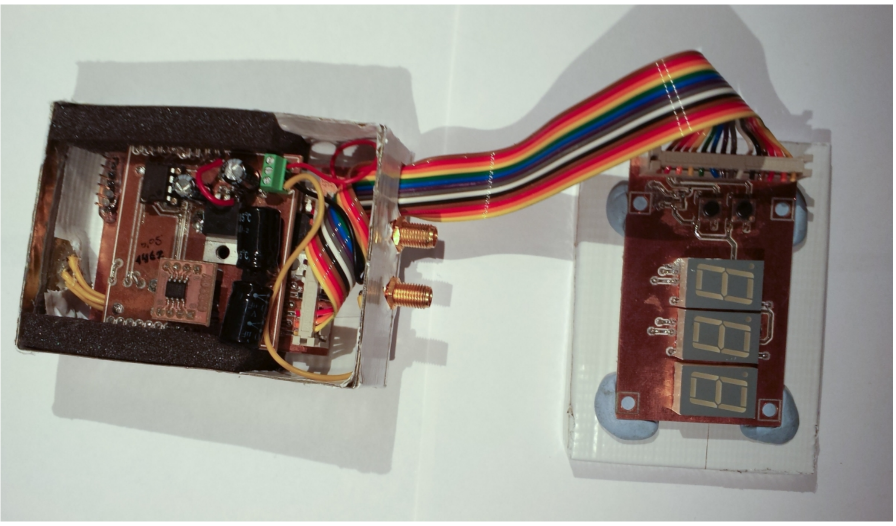

Figure 4.10: Device, connected and enclosed

Shunt probes from the drill are inserted to the SMA connectors, such that **probe with the copper band around it goes to the connector closer to the USB slot**. It is preferable to mount the device on the drill and plug the probe cables in before inserting the battery into the drill.

Measurement program

Instrument program combines routines for ADC sampling, signal filtering, computing the linear torque model and multiplexing the result onto display.

Readings, gathered from the ADC channel are collected and averaged 1024 samples at a time. Each second, filtered value is refreshed and multiplied by fixed coefficient K_t.

Figure 4.11: Drill with the device and shaft coupler

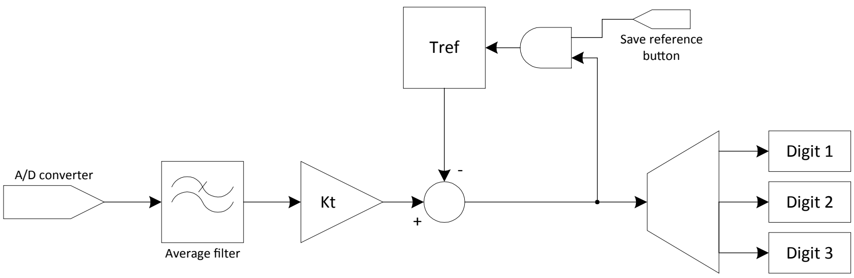

Figure 4.12: Measurement program

It is possible to set the reference T_{ref}, being constant component of the linear model, by pressing the upper button on the display board. Similar kind of reference button functionality can be observed on digital scales. This allows to easily display braking torque which is relative to the desired reference.

Multiplexing algorithm works by time-division principle. It splits the final torque value to separate digits and maps it to the 7-segment bus. Briefly displaying the digit on the screen, it switches power to the second screen, mapping another value on the bus.

Programming interface

Programing and debugging is the cornerstone of the design workflow. The programming part consists of writing code and uploading it to the μC. For the MSP430 there are several options: open-source GCC tool chain, professional IDE like Code Composer Studio and IAR, and TI provided Energia studio. The initial design used IAR studio, but the limitations in free version forced us to switch to Energia.

Over the years there were tools developed to help developers to see what is happening inside the μC. The industry and IEEE standard for that is the JTAG interface. It provides features like breakpoints, step-by-step execution, direct access to memory. However, the problem is JTAG requires 4 wires for it's operation, which could be problematic for smaller microcontrollers.

As a workaround Texas Instruments offers their own implementation: Spy-Bi-Wire (SPB). Essentially, SPB is just serialized JTAG and provides most of JTAG features using only 2 wires at the cost of lower speed. On the μC board, there is a 6-pin connector near the edge. The pinout goes starting from black wire: GND, TEST, RST/SBWTDIO, RXD, TXD, VCCdebug.

GND is the common ground; TEST is the clock signal; RST/SBWTDIO is the bidirectional data signal; RXD and TXD and receiving and transmitting lines for UART interface; VCCdebug is the electrically isolated power line.

The routing of the board is made in a way that allows μC to use different power supplies using the switch at the front side. In normal condition, there is no power at the VCCdebug and the switch works as the power switch. When debugging interface is connected, you can use it to switch between power supplies.

To reprogram the μC, use the following routine:

1. Disconnect the battery.
2. Take off the cap.
3. Plug the programming interface into your PC or laptop.

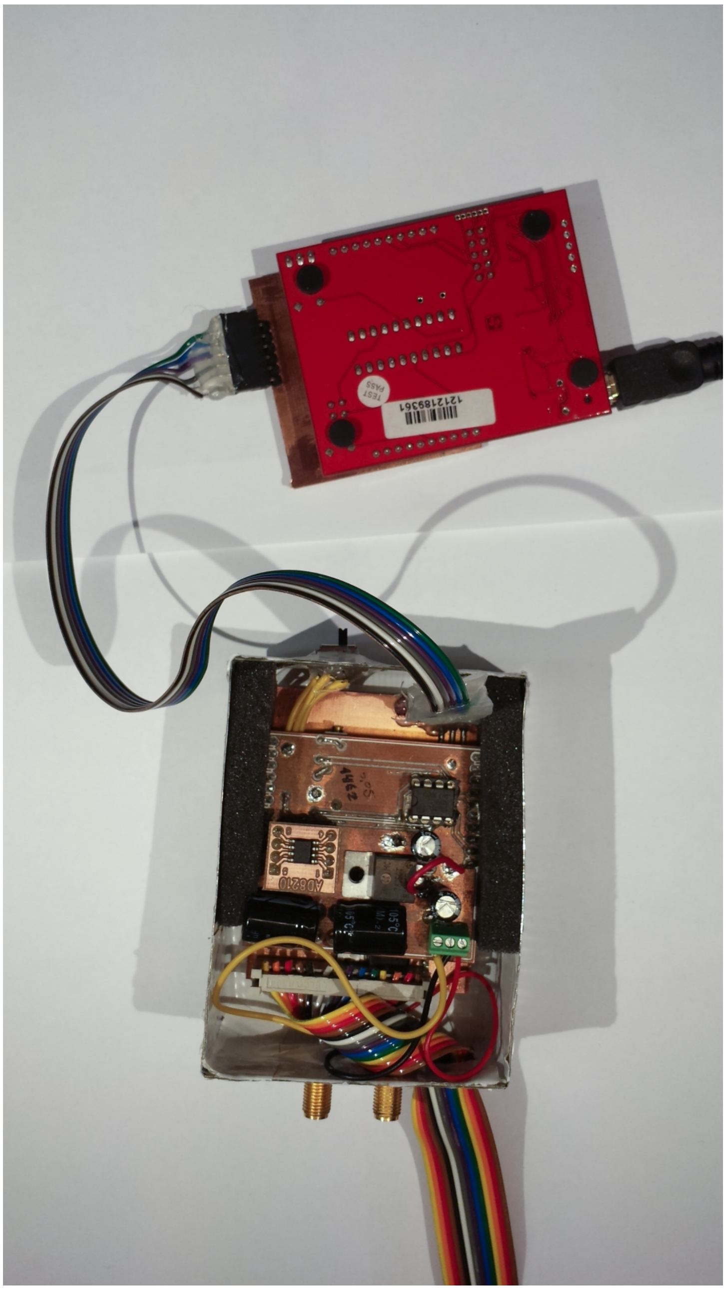

Figure 4.13: Programming interface connected to the μC board

4. Plug in the connector into the socket on the μC board. Near the socket there is a black dot. It indicates the GND line. Plug in the connector so that the black wire in the ribbon cable is aligned with the black dot.
5. Now the programming interface should be recognized by the system. *Slightly* push the socket towards the center of the board and press 'Program'.
6. Unplug the connector, put the cap on and connect the battery back.

Calibration

During the whole design process the device had to be calibrated and recalibrated to make sure it follows the specifications given. When the project approached its final state, the power supply was switched from the one provided by the Launchpad to LM350. As the result, the VCC changed slightly and as ADC measures voltage in fractions from Vgnd to Vcc, the output values also changed slightly hence the device had to be recalibrated.

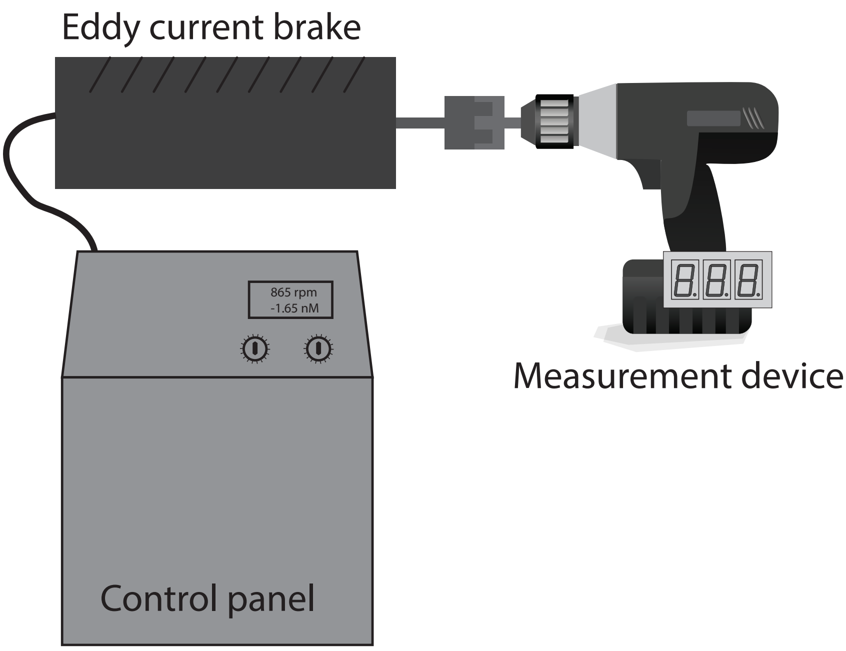

Figure 4.14: Setup of the recalibration procedure

Metropolia AMK provided a mechanical lab to conduct the measurements. The following setup was used: The drill was connected through a mechanical coupler to an eddy current brake. The brake is connected to the control panel, which shows the negative torque generated by the brake and also allows to tune it. A Nikon

Figure 4.15: Calibration procedure

DSLR camera was used to record the control panel and the measurement device at the same time. Later these values were collected, averaged, plugged into MATLAB to generate the plot and the curve fitting equation.

The process goes in the following way:

- The drill is turned on, generating the torque.
- When the torque stabilizes, the 'set reference' button is pressed to account for all the losses in the drill, coupler and eddy current brake.
- Using the control panel, certain amount of negative (braking) torque is applied to the drill.
- The values are recorded, the previous step is repeated until enough data is collected.

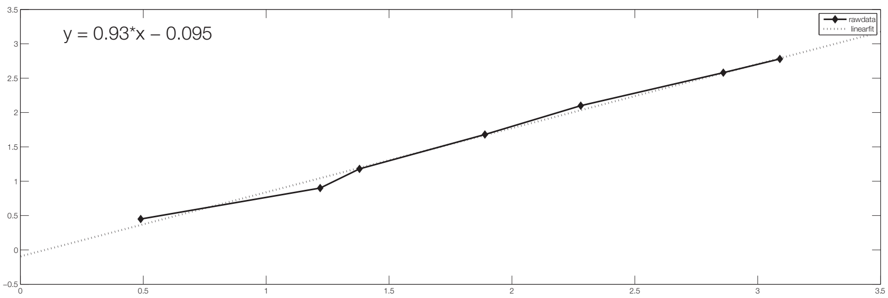

Figure 4.16: Raw data (Drill values vs. actual values) and linear fit

It became apparent that our values are off by ~7.5% and the coefficient must be multiplied by 0.93.

5 Performance tests

ABB test

Finally, a performance test has been carried out in the ABB factory. To connect the cordless drill to the insulation machine tape holder, special type of coupler was used. In the test, two different tape rolls with corresponding diameters of 50 mm and 82 mm were inserted into tape holder. Braking torque then was measured for each tape roll. Criteria of the taping head performance is the tension force of about 60 N in magnitude, applied to the tape during insulation process. Tension should be constant throughout whole roll unwinding, so that for small and for big roll brakes are supposed to deliver approximately same amount of torque (see Introduction).

Nominal rotation of the taping head is 200 RPM. HIGH gear of the drill typically delivers 1400 RPM, which causes exceptional overheating of the taping brakes. Because of this, measurement was made with LOW gear of the drill, which corresponds to nominal of 400 RPM.

Figure 5.1: Measurement with small tape roll

From the pictures, following torque values can be seen: 0.47 Nm for small tape roll and 1.11 Nm for a big tape roll. These values should be scaled for the mechanical advantage of different drill speed setting. Gear ratio is approximated as ratio between nominal rotation speeds:

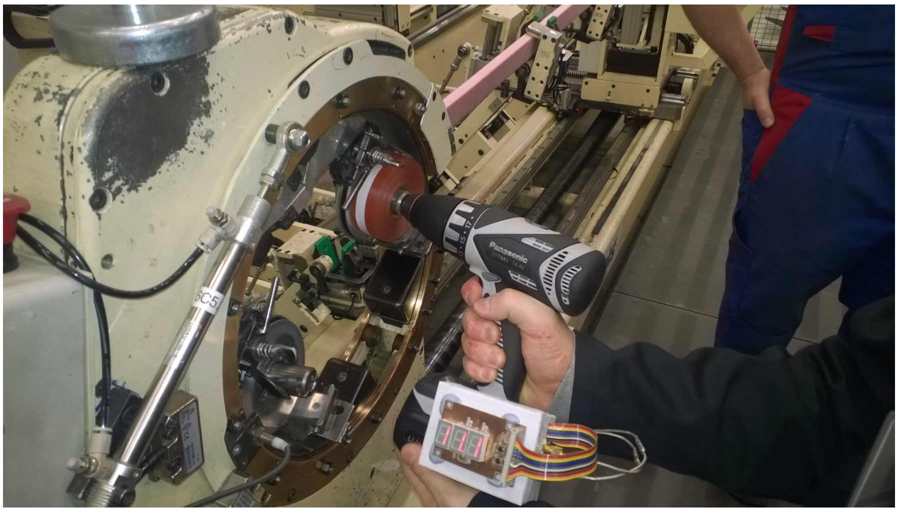

Figure 5.2: Measurement with big tape roll

$$R = \frac{T_2}{T_1} = \frac{\omega_1}{\omega_2}$$

$$R = \frac{1400}{400} \Rightarrow T_2 = 3.5 \cdot T_1$$

Thus, torque read from calibrated device is to be compensated by factor 3.5. Resulting values should be additionally divided by the lever-arm length (diameter of the tape roll) to find the force for the small and big rolls accordingly:

$$\frac{0.47[Nm] \cdot 3.5}{0.025[m]} = 65.8[N]$$

$$\frac{1.11[Nm] \cdot 3.5}{0.041[m]} \approx 94.6[N]$$

According to the measurement, tape tension is not constant with different roll diameters, and brakes barely match the expected performance criteria. Mismatch of the results with expectations may happen because of following factors:

- Unusual brake heating due to twice as fast rotation speed compared to nominal
- Poor gear ratio approximation
- Non-linearity of taping brake adjuster
- Initial brake calibration is unknown

Measurement quality can be improved by approaching to the actual operating conditions. Sensing device should be recalibrated for lower rotation speeds, as well as dynamic range of the torque should be fixed to about 1.5 Nm. Latter is possible by adjusting the gain trimmer on the signal preconditioning board.

EMC Emission test

EMC scan with an EMC scanner and near field probe of the torque measuring device was done. The electromagnetic emission amplitude in dBμV was measured using the EMC scanner, spectrum analyzer, and the appropriate software. The software detects in which frequencies the emission limits of the device are exceeded and creates a 3 dimensional graph of the emission amplitude at the scanning frequency.

Equipment used:

- DETECTUS DS642 EMC scanner
- HP11941A close field probe (9 kHz - 30 MHz)
- HP11940A close field probe (30 MHz - 1 GHz)
- ROHDE & SCHWARZ 9 kHz … 13.6 GHz Spectrum analyzer

The emission measurement is done twice as two near field probes for different frequency regions are used. First a pre-scan is done to detect the frequencies at which the emission amplitude exceeds the specified limits after which it can be specified at which frequencies the full EMC scan is done. The following image shows the scanner table and the tested device positioned on it.

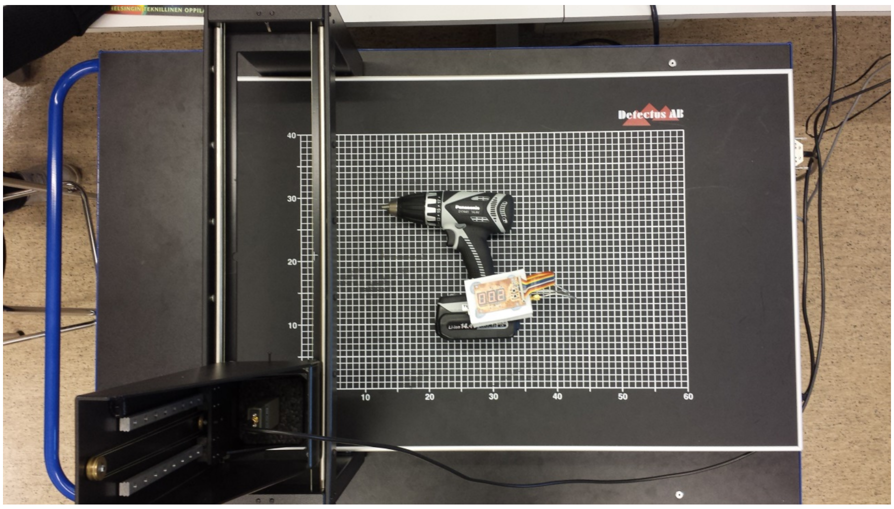

Figure 5.3: EMC scanner table with the tested device

The measurement of the device was done so that the torque measuring device was connected to the drill and turned on, but the drill was not turned on as the purpose of this test was to measure the emissions of the torque measuring device not the drill.

Pre-scan of the device to determine the frequencies at which the limits are exceeded:

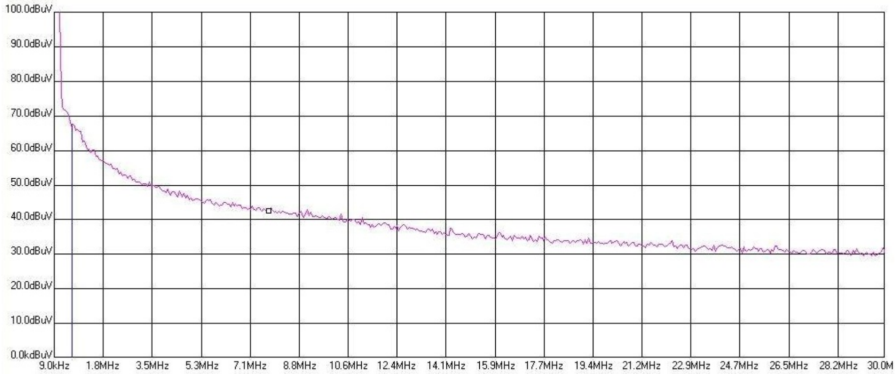

Figure 5.4: Emission amplitude in dBµV over the frequency range of 9 kHz - 30 MHz

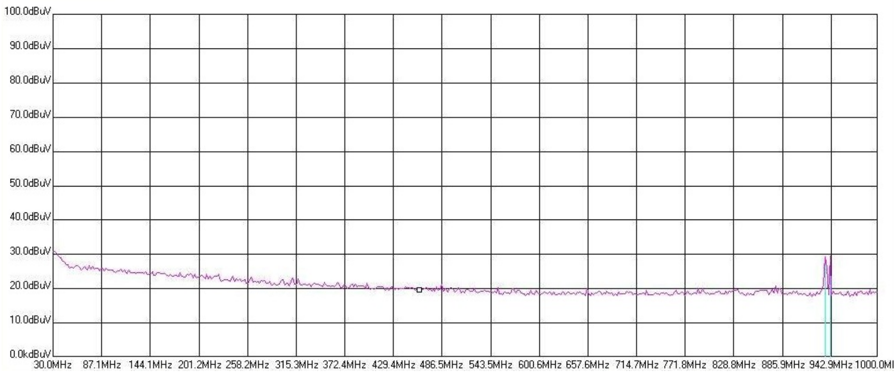

Figure 5.5: Emission amplitude in dBµV over the frequency range of 30 MHz - 1 GHz

A peak closer to 0 Hz can be observed in the low band. It must be noted that this peak is internally generated due to the VCO (voltage controlled oscillator) in the spectrum analyzer and is present even if no input signal is present. Two spikes in radiated emissions were found at frequencies of 936 MHz and 942 MHz. These are emissions not from the tested device but from the communication network. It can be proven by simply repeating the measurement without the device and it will be seen that the emissions at around those frequencies will still be present. By observing the emission amplitude level over the rest of the frequency range it can be seen that there is no notable emissions from the device.

6 Possible further development

In order to maximize usefulness of the torque meter in the stator coil manufacturing process, and improve overall operator experience, measurement device can be refined for this particular purpose, based on already developed concept. Following improvements can be done:

- Filtering of the input signal with multi-stage active filters.
- Cleaning of the shunt voltage with DSP algorithms implemented on a microcontroller with relatively fast ADC.
- For the taping machine torque range, gain of the shunt signal implemented with fixed components.
- Integration of motor PWM current with analog circuit or with DSP algorithms (thus allowing for lower drill RPM).
- Monitoring the battery charge level with auxiliary ADC input and a battery specific look-up table.

By applying these techniques, is possible to reduce the size of the device to a small board, especially if narrow footprint SMD components are used.

7 Conclusion

In this project, we have successfully proven the proposed concept of braking torque measurements. Drilling machine has been examined and modified such that future changes and improvements can be introduced to the system. Drill motor performance has met theoretical model predictions and was successfully modelized. As a result, detachable electronic device allows for general torque measurements with the drill.

Industrial tests went fluently and have been partly satisfactory. At this point, further development of the device should take closer approach to the actual application. Maximum precision inside coil taping machine operating limits can be achieved with various improvements.

8 References

[1] M. Gopal. Control systems: principles and design. 2nd ed. Tata McGraw-Hill, 2002. Page 162.

[2] Texas Instruments MSP430G2553 datasheet